Theoretical Studies on the Catalytic Activity of Ag Surface for the Oxidation of Olefins

HIROSHI NAKATSUJI,[1,2,3] ZHEN-MING HU,[1] HIROMI NAKAI[1,*]

[1]*Department of Synthetic Chemistry and Biological Chemistry, Graduate School of Engineering, Kyoto University, Sakyo-ku, Kyoto 606-01, Japan*

[2]*Department of Applied Chemistry, Graduate School of Engineering, University of Tokyo, Hongo, Tokyo 113, Japan*

[3]*Institute for Fundamental Chemistry, 34-4, Takano-Nishihirakicho, Sakyo-ku, Kyoto 606, Japan*

Received 2 March 1997; accepted 14 March 1997

ABSTRACT: Systematic theoretical studies for the mechanisms of the epoxidation and complete oxidation of ethylene and propylene over silver surface as well as the reactivity and the stability of oxygen species on Cu, Ag, and Au surfaces have been presented. The dipped adcluster model (DAM) combined with the ab initio Hartree–Fock (HF), second-order Møller-Plesset (MP2), and SAC/SAC-CI (symmetry-adapted cluster/configuration interaction) methods are used. These studies clarify the origin of silver as a unique effective catalyst for the epoxidation of ethylene and the different mechanisms for the oxidation of olefins over silver surface. For the epoxidation of ethylene, the superoxide O_2^-, which is molecularly adsorbed in bent end-on geometry on the silver surface, is the active species. The origin of the unique catalytic activity of silver for the epoxidation of ethylene is due to its ability to adsorb oxygen as the superoxide species. Such an adsorbed species cannot be stable or exist on Cu and Au surfaces. For the oxidation of propylene, both reaction mechanisms initiated by the activation of olefinic carbon and by the activation of the allyl hydrogen exist. The activation of the allyl hydrogen is the origin of the complete oxidation of some olefins over silver surface. The present results not only let us have a better understanding of the reaction mechanisms of olefins over silver surface but also supply a basic idea for the new catalyst design of the epoxidation reaction. Int J Quant Chem **65**: 839–855, 1997

* *Present address*: Department of Chemistry, School of Science and Engineering, Waseda University, Ohkubo 3-4-1, Shinjuku-ku, Tokyo 169, Japan.

Correspondence to: H. Nakatsuji.

Contract grant sponsor: Japanese Ministry of Education, Science, and Culture and the New Energy and Industrial Technology Development Organization (NEDO).

CCC 0020-7608 / 97 / 050839-17

Key words: Reaction mechanism; epoxidation; combustion; catalytic activity of silver, copper, and gold; superoxide; atomic oxygen; propylene; ethylene; dipped adcluster model (DAM); SAC/SAC-CI method; ab initio Hartree–Fock (HF) and second-order Møller-Plesset (MP2) methods

Introduction

The heterogeneous selective oxidation of olefins to epoxides on silver

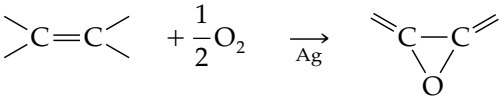

olefin epoxide (1)

is an exceedingly important industrial catalytic reaction, and as such has received long and extensive study [1–7]. One particularly interesting aspect of the epoxidation reaction is its uniqueness: Not only is silver a uniquely effective catalyst for heterogeneous epoxidation but also ethylene is the only hydrocarbon which may be epoxidized with high selectivity. Actually, silver catalysts are used in industry to produce several million tons of ethylene oxide yearly [1–4]. Recent experimental studies show that, except for ethylene, only a few olefins such as styrene [8, 9], 3,3-dimethylbutene [10], norbornene [11], and butadiene may be epoxidized over silver with high selectivity. In contrast, other olefins such as propylene, butenes, and pentenes are epoxidized over silver but with extremely low selectivity [12–16].

During the past 20 years, many studies [12–24] have been devoted to getting a better understanding of the epoxidation reaction mechanism. However, the origin of this unique catalytic activity of silver has not yet been clarified, and also the mechanistic details of the epoxidation and that of the competing combustion to carbon dioxygen and water are far from understood. One of the main questions about the mechanism of ethylene oxidation is the roles of the adsorbed molecular and atomic oxygen. Both mechanisms involving molecular oxygen [12–18] and atomic oxygen [19–23] as the active species have been suggested. It has been suggested that the uniqueness of silver is associated with its ability to adsorb oxygen as the superoxide species [24]. More direct evidence for molecular oxygen as the active species has been obtained by several studies: e.g., only complete oxidation occurs when N_2O pulse which gives atomically adsorbed oxygen is used, but the epoxidation reaction occurs when O_2 pulse which gives molecularly adsorbed oxygen, at least initially, is used [25]. The mechanism assuming atomic oxygen as an active species was suggested from the experimental data that only atomically adsorbed oxygen exist at high temperature in an industrial condition, since molecular oxygen desorbs or dissociates. The assumption that molecular and atomic oxygens cause the partial and total oxidation reactions, respectively, gives an upper limit for the selectivity of 6/7. Recent experiments giving higher selectivity than 6/7 [26] imply that the atomic oxygen may at least pay an important role for the epoxidation of ethylene.

Theoretical studies have done much less for the epoxidation reaction of olefins. Though a few works [27–30] studying the epoxidation mechanism of ethylene have ever been published, less discussions were presented [27, 30] for the oxidation of propylene, and the calculations did not explicitly include the surface contribution. The main difficult problem still remaining in the theoretical studies is how to describe chemisorption species and calculate adsorption energy correctly based on a selected small cluster. This may be why no ab initio theoretical study for the full reaction pathway and the associated energy diagrams of the epoxidation reaction of olefins has been reported.

In a series of our previous studies [31–37], a theoretical model, named the dipped adcluster model (DAM) [31–33], has been proposed to study chemisorptions and surface reactions by involving the interactions between bulk metal and admolecules with consideration of the electron transfer between them and the image force correction. Such an interaction is found to be very important for studying the chemisorptions and the reactions of the oxygen on a metal surface, and even a small DAM could be used to give correct electronic

structures and reliable adsorption energies in contrast to the cluster model. Previous studies [34–36] for the chemisorption of oxygen on a silver surface showed that the molecularly adsorbed oxygen exists in two stable geometries; i.e., an end-on (bent) structure in an on-top site and a side-on structure in a bridge site. The ground state in the former geometry is superoxide, which is expected to be more electronically favorable for the reaction with ethylene [36].

In this work, we present a brief account of our recent systematic studies on the catalytic activity of silver surface for the oxidation of olefins. We will try to address the following three questions: (1) What species of surface oxygen is responsible for the ethylene epoxidation? (2) Why is silver a unique catalyst for the epoxidation? (3) Why do higher olefins mainly process complete oxidation on the same silver catalyst? We performed the ab initio Hartree–Fock (HF), second-order Møller-Plesset (MP2), and the SAC (symmetry-adapted cluster)/SAC-CI (configuration interaction) calculations with the use of the DAM. More details are seen in the literature [38–40].

Epoxidation Mechanism of Ethylene on Silver Surface

In this section we give an account of our research on the mechanism of the epoxidation of ethylene on a silver surface [38]. The energy diagrams of the reactions of ethylene with both molecularly adsorbed and atomically adsorbed oxygens on a Ag surface are studied. The Eley-Rideal mode, namely the reaction between the adsorbed oxygen species and a gaseous ethylene is assumed. The DAM was used to include the effects of the bulk metal such as the electron transfer between adcluster and surface and the image force. Geometry optimizations for calculating the reaction path were performed using the ab initio unrestricted Hartree–Fock (UHF) method and the energies at the optimized geometries were calculated by the MP2 methods including the image force correction. The Gaussian basis set used is of double-zeta accuracy, and some additional functions were added for improvement. They are shown to reproduce well the known geometries and the energetics of the reactions [38]. The model adclusters used in the present study are the molecularly adsorbed end-on (bent) form in an on-top site and the atomically adsorbed on-top structure.

REACTIONS WITH MOLECULARLY ADSORBED OXYGEN

Epoxide Formation

We first study the epoxidation reaction of ethylene with the molecularly adsorbed superoxide on a silver surface. For the formation of ethylene oxide, the reaction takes place by an initial interaction of the oxygen with one of the carbon in ethylene [5, 6]. Figure 1 shows the obtained favorable initial attack of ethylene to superoxide species adsorbed on the silver surface. Starting from this geometry, we optimized the geometries of the intermediates and the transition states (TSs) along the reaction pathway. The optimized geometries and energy diagrams are shown in Figure 2. The reaction proceeds from the left to the right, and the energy is in kcal/mol relative to the free system, i.e., $Ag_2 + O_2 + C_2H_4$.

Figure 2 shows a two-step mechanism of the reactions. The first step of this reaction is the adsorption of molecular O_2 on Ag surface in which one electron is transferred from the bulk metal to the adcluster, i.e., $n = 1$. The transferred electron mainly occupies the out-of-plane p^* orbital of O_2, and the in-plane p^* molecular orbital (MO) of O_2 remains singly occupied. The ground state for the end-on adsorption of O_2 is the superoxide. The adsorption energy of superoxide is calculated to be

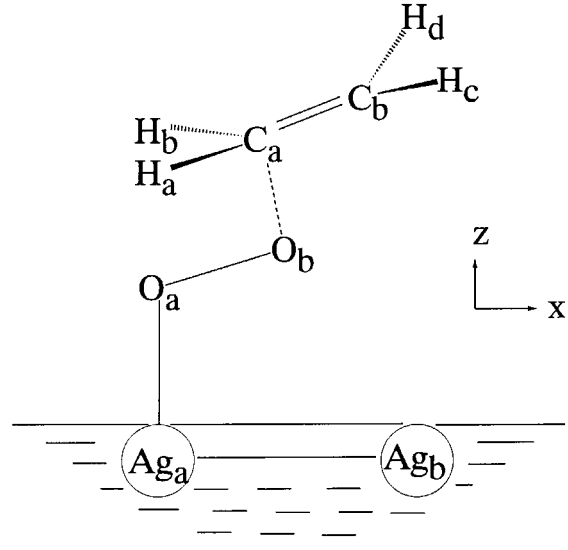

FIGURE 1. Model adcluster used. Geometries were optimized in the Cs symmetry except for the Ag — Ag distance and the O_a — Ag — Ag angle fixed at 2.8894 Å and the 90.0°, respectively.

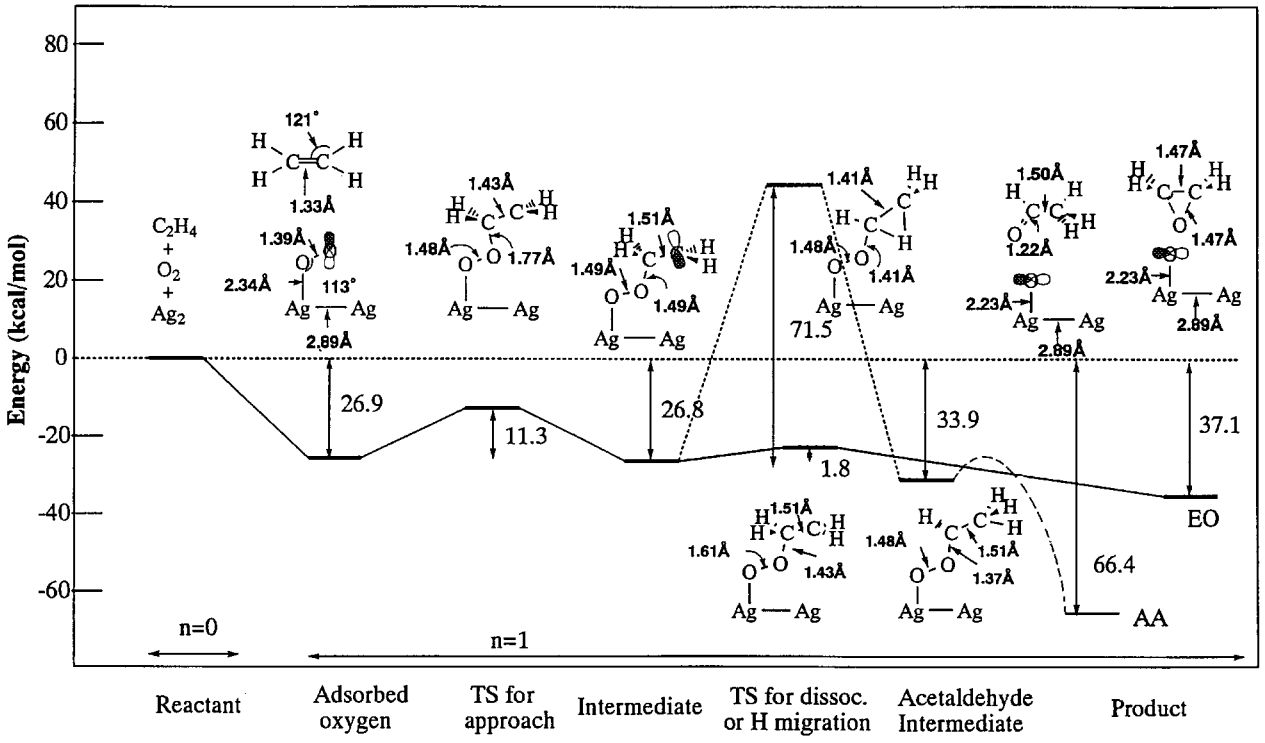

FIGURE 2. Energy diagram for the reaction between ethylene and molecularly adsorbed superoxide on Ag surface. The route leading to ethylene oxide (EO) and acetaldehyde (AA) are shown by the solid and broken lines, respectively.

7.4 kcal/mol at the UHF level and 26.9 kcal/mol at the MP2 level. The experimental molecular adsorption energies are 9.2, 9.3, and 24.1 kcal/mol for the Ag(111) [18], Ag(110) [18], and electrolytic Ag [41] surfaces, respectively. The next step is the attack of ethylene onto the terminal oxygen atom O_b which is more reactive than the inside one O_a, leading to the TS and the intermediate with the energy barrier of 11.3 kcal/mol. The energy level of the intermediate is similar to that of initial step. In the TS the σ bond between O_b and C_a is formed and the in-plane p bond of O_2 and the p bond of C_2 are broken. The geometry parameters at every step clearly reflect the reaction processing along the reaction path [38].

When the intermediate is produced, the formation of ethylene oxide is an easy path as shown by the real line, leaving an atomic oxygen on the Ag surface. The calculated heat of reaction is 37.1 kcal/mol. The energy diagram given in Figure 2 shows that the reaction leading to ethylene oxide proceeds very smoothly: The reaction is exothermic, there are no very high barriers, and there are no too stable intermediates. We therefore conclude that the epoxide formation reaction from the superoxide species on a silver surface proceeds very smoothly. We note that the exothermicity of the overall reaction is partially due to the formation of the atomically adsorbed oxygen on the silver surface.

Acetaldehyde Formation

We next study the formation process of acetaldehyde from ethylene and molecularly adsorbed superoxide on the Ag surface. In Figure 2, the path is given by the broken line. When acetaldehyde is produced, it is further oxidized to CO_2 and H_2O by combustion in the presence of adsorbed oxygen, and therefore it is an intermediate in the complete oxidation process [42].

The formation of acetaldehyde starts from the intermediate shown in the center of Figure 2: up to it the reaction path is common to the epoxidation reaction. H_a bound to C_a in the intermediate migrates to C_b, giving a stable conformation denoted as acetaldehyde intermediate in Figure 2. However, the energy barrier for this H_a migration is as high as 71.5 kcal/mol. This step is therefore energetically forbidden. This is a reason for the high

selectivity of the epoxide formation process starting from the superoxide species summarized in the preceding section.

Effect of Silver Surface

The effect of the silver surface may be twofold: One is to provide a reactive species adsorbed on the surface, and the other is to provide electrons to the reaction site as considered in the DAM. Figure 3 shows the energy diagram for the reaction between ethylene and gaseous oxygen without the silver surface. Two energy diagrams correspond to the calculations with $n = 1$ and $n = 0$. The former involves an excess electron but the latter is neutral. For $n = 1$, we used the optimized geometries shown in Figure 2, and, for $n = 0$, we performed the geometry optimization for the present purpose. The geometries illustrated in the upper and lower sides correspond to those for $n = 0$ and $n = 1$, respectively. For $n = 0$, the O—O distance is calculated to be 1.37 Å for the intermediate, which is smaller than the corresponding value 1.49 Å for $n = 1$. The same is true for all the intermediates and TSs.

Comparing Figure 3 with Figure 2, we clearly see the catalytic activity of the silver surface for the epoxidation reaction. Without the surface, the reaction is endothermic and the pathway has a large barrier. Electron transfer ($n = 1$) certainly reduces the barrier, but the direct interaction with the actual silver atoms on the surface is quite important. Clearly, the exothermicity of the reaction shown in Figure 2 is due to the formation of the atomically adsorbed oxygen on the surface.

REACTIONS WITH ATOMICALLY ADSORBED OXYGEN

When ethylene oxide is ejected out of the Ag surface, the atomically adsorbed oxygen O^- is left on the surface. It is also produced by the dissociative adsorption of O_2 on the surface, and the dissociative state is more stable than the molecular adsorption state. In our calculation, the dissociated oxygen has its singly occupied orbital in the $2p$ orbital parallel to the surface.

Figure 4 shows the energy diagram for the reaction of ethylene with the atomically adsorbed oxygen on the Ag surface. When ethylene attacks

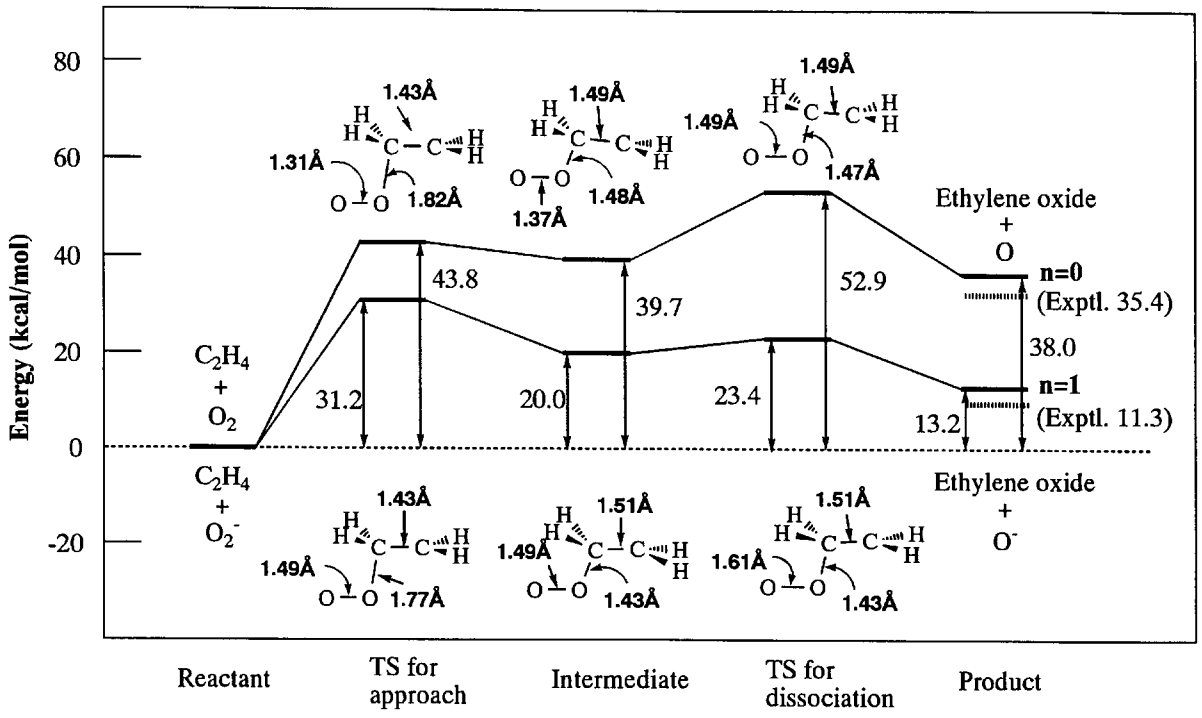

FIGURE 3. Energy diagram for the reactions between ethylene and gaseous oxygens [neutral O_2 ($n = 0$) and O_2 anion ($n = 1$)]. The upper geometries are for $n = 0$, and the lower geometries for $n = 1$.

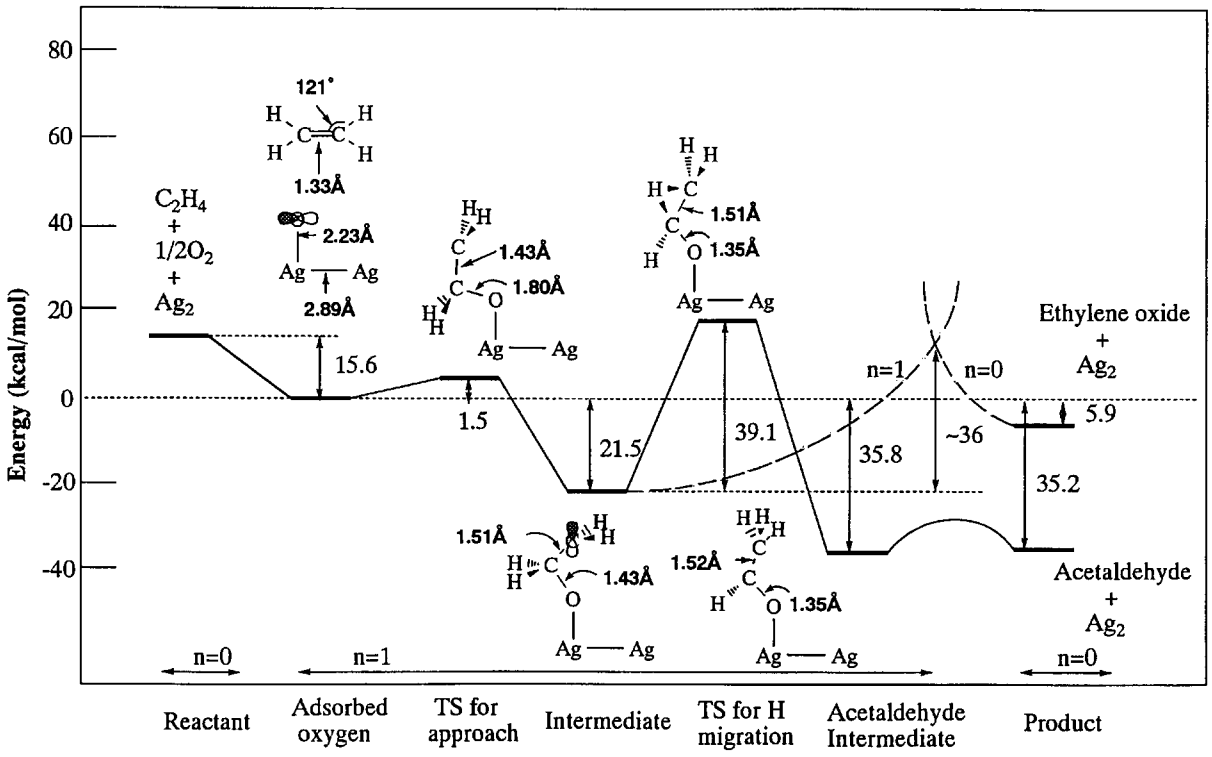

FIGURE 4. Energy diagram for the reaction between ethylene and atomically adsorbed oxygen on Ag surface.

atomic oxygen on the surface, the most favorable approach is to form the C_a—O_a bond as illustrated in Figure 4. It is similar to the approach of ethylene to the superoxide species shown in Figure 2. The calculated energy barrier from the adsorbed oxygen to the intermediate is, however, as small as 1.5 kcal/mol, reflecting the reactivity of the atomic oxygen.

The next step from this intermediate is very important, since it determines the selectivity of the atomically adsorbed oxygen. If C_b attacks the oxygen to form the C_b—O_a bond, ethylene oxide is formed. If C_b attacks another C—H bond, causing the hydrogen migration, acetaldehyde is a product, which is an intermediate for the complete oxidation product.

For the hydrogen migration reaction, the barrier was calculated to be 39.1 kcal/mol, which is high but lower than the barrier, 71.5 kcal/mol, of the reaction in which the superoxide species was involved (see Fig. 2). This process were calculated using the adcluster with $n = 1$. Unfortunately, the structure of the TS to form the C_b—O_a bond could not be determined by the geometry optimization procedure using both of the $n = 1$ and $n = 0$ adclusters. If the pathway from the intermediate to ethylene oxide is one step, it is a quite interesting step since it involves both geometrical changes and *one electron back-transfer* from the admolecule to the bulk metal. In the DAM picture, the intermediate in Figure 4 is neutrally described with $n = 1$, i.e., with one additional electron supplied from the bulk metal to the adcluster, but the product, ethylene oxide plus Ag_2 should be neutral, i.e., $n = 0$. Therefore, we calculated two potential curves, one starting from the intermediate and the other from ethylene oxide plus Ag_2 using $n = 1$ and $n = 0$, respectively. All the geometrical parameters were assumed to change linearly, except for the Ag—O distance, which was fixed to 2.180 Å.

The potential curve for $n = 1$ increases monotonically from the intermediate to the product, while the curve for $n = 0$ also increases monotonically from ethylene oxide and Ag_2 to the intermediate, and the two energy curves cross. The energy difference between the crossing point and the intermediate is about 36 kcal/mol, which may be considered as the energy barrier of this process. Namely at this TS, one electron is transferred back to the metal.

The selectivity giving either ethylene oxide or acetaldehyde would be dependent on the heights of the barriers of the two processes and on the stabilities of the two products. The calculated energy barriers for the two processes are similar, 39.1 and about 36 kcal/mol, respectively. On the other hand, the energy difference between the two products and the intermediate are +15.6 and −13.7 kcal/mol, respectively, which means endothermicity and exothermicity from the intermediate, respectively. From the above data alone, it is difficult to decide which is a preferential process, though the acetaldehyde formation may be favorable for the exothermicity. However, it may be said that both ethylene oxide and acetaldehyde are formed from ethylene and atomically adsorbed oxygen on the Ag surface. Furthermore, this fact is very important since it would be a reason for the experimental maximum selectivity more than 6/7 [5–7].

OVERALL MECHANISM OF EPOXIDATION OF ETHYLENE

We summarize here our results on the mechanism of the epoxidation of ethylene on a silver surface. The calculated energy barriers and the heats of the reactions are summarized in Table I. The primarily important species for the epoxidation of ethylene on a silver surface is the superoxide O_2^- which is molecularly adsorbed on the surface in the bent end-on geometry. Ethylene attacks the terminal oxygen atom of the superoxide, as shown in Figure 1, with the barrier of about 11 kcal/mol, and then the reaction proceeds quite smoothly leading to ethylene oxide as shown in Figure 2. The overall reaction is exothermic by 37 kcal/mol from $C_2H_4 + O_2 +$ Ag surface or by 10 kcal/mol from $C_2H_4 +$ superoxide on Ag surface. The second exothermicity is due to the larger adsorption energy of the atomic oxygen than that of the superoxide.

On the contrary, the complete oxidation of ethylene from the superoxide species is forbidden due to the existence of the large barrier (72 kcal/mol) in the hydrogen migration step, though this reaction is largely exothermic by 66 kcal/mol from the initial compounds or by 40 kcal/mol from the superoxide on Ag and C_2H_4. When silver surface does not exist, the epoxidation reaction is a very unfavorable reaction having a high-energy barrier and endothermicity. Thus, the epoxidation of ethylene by the superoxide on the Ag surface is highly efficient and selective.

The atomically adsorbed oxygen, which is left on the surface after completion of the epoxidation reaction by the superoxide or which may exist by the dissociative adsorption of O_2 on the surface, has two reaction channels leading to ethylene oxide and to complete oxidation. The selectivity here seems to be small and both products would be obtained. This would be the reason why some experiments reach the selectivity larger than 6/7.

In the process leading to ethylene oxide, the electron back-transfer from the reaction adsorbate complex to the metal surface should be important and related to the barrier. We note that both electron acceptor and donor may work to reduce the barrier of the electron transfer step: They work to stabilize the $n = 1$ and $n = 0$ curves, respectively. The effects of Ce and halogen as promoters of catalyst are well known experimentally [5–7]. We

TABLE I

Comparison of the energy barrier and the heat of reaction for the epoxidation and acetaldehyde formation by the molecularly and atomically adsorbed oxygens (kcal / mol).

Reaction	Energy barrier	Heat of reaction[a]
Molecularly adsorbed oxygen		
$O_2(a)$ / Ag + $C_2H_4 \rightarrow C_2H_4O + O(a)$ / Ag	11.3	10.2
$O_2(a)$ / Ag + $C_2H_4 \rightarrow CH_3CHO + O(a)$ / Ag	71.5	39.5
Atomically adsorbed oxygen		
$O(a)$ / Ag + $C_2H_4 \rightarrow C_2H_4O$ + Ag	~36	21.5 (24.7)
$O(a)$ / Ag + $C_2H_4 \rightarrow CH_3CHO$ + Ag	39.1	50.8 (52.3)
Without Ag surface		
$O_2^- + C_2H_4 \rightarrow O^- + C_2H_4O$	31.2	−13.2 (−11.3)
$O_2 + C_2H_4 \rightarrow O + C_2H_4O$	52.9	−38.0 (−35.4)

[a] Values in parentheses show the experimental values.

speculate that these promoters act in this electron-transfer step. Design of the promoter or co-catalyst, which is effective to this electron-transfer step, is of crucial importance since it would be a key for raising up the selectivity over 6/7.

Activation of O_2 on Cu, Ag, and Au Surfaces

The experimental results show that silver is a unique catalyst for the epoxidation of ethylene. However, it is not yet well understood why only silver is so exceptional. In the former section, we showed that the superoxide species adsorbed in the end-on form on a Ag surface is very active and selective for the epoxidation reaction. Aiming to clarify the reason why only silver is an effective catalyst for the epoxidation of ethylene, in this section, we perform a comparable study for the chemisorption and activation of oxygen on Cu, Ag, and Au surfaces.

We take M_2O_2 (M = Cu, Ag, Au) as adclusters. Both electronic structures and the reactivity of the molecular end-on and side-on adsorptions are studied. The geometries of the molecular end-on and side-on species are optimized at the UHF level. The relative stabilities of the adsorbed species is studied by SAC/SAC-CI method [43–45], since the roles of lower ground and excited states are quite important in this kind of surface electronic processes [34–36]. The DAM [31–33] is again adopted to investigate the electron transferability of these surfaces.

REACTIVITY AND STABILITY OF SUPEROXIDE SPECIES

Figure 5 shows an illustration of the geometries of the end-on and side-on forms. The calculations are performed by assuming one-electron transfer from the bulk to the adcluster occurs. The optimized O—O distances are 1.36–1.38 Å in the end-on form, which are close to or slightly greater than that of a free O_2 anion (1.35 Å) [46], and that in the side-on form are all about 1.51 Å. The calculated Cu—O distance are shorter than the Au—O and Ag—O distances, reflecting a large adsorption energy and a short lattice constant of Cu.

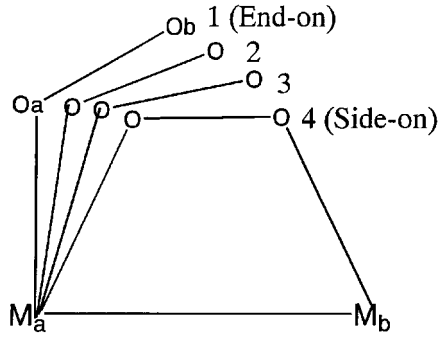

FIGURE 5. Illustration of the geometrical conversion from end-on (#1) to side-on (#4) forms. The M — M (M = Cu, Ag, and Au) distances were fixed at the lattice constants.

The calculated electronic structure of O_2 in the end-on and side-on adsorption forms is superoxide O_2^- and peroxide O_2^{2-}, respectively. Table II shows the net charge and frontier density (or spin population), which are related to the reactivity of the superoxide species. In all three species, the net charges on the inside (O_a) and outside (O_b) oxygen atoms are calculated to be about -0.6 and -0.15, respectively, while the outside oxygen atoms have a frontier density of about 0.86, which is much larger than that of the inside oxygen atoms (about 0.12). This shows that the outside oxygen is much more reactive than the inside one and that the former is not so negative as the latter one, the same result as that reported before [36] for a linear Ag—O—O system. Actually, in the epoxidation reaction with ethylene, the oxygen that reacts with

TABLE II
Net charge and frontier density of the end-on superoxide species on Cu, Ag, and Au surfaces.

	Net charge				Frontier density			
System[a]	M_a	M_b	O_a	O_b	M_a	M_b	O_a	O_b
Cu_2O_2	+0.060	−0.271	−0.643	−0.146	0.007	0.002	0.133	0.858
Ag_2O_2	+0.058	−0.295	−0.605	−0.158	0.014	0.003	0.119	0.864
Au_2O_2	+0.095	−0.285	−0.644	−0.166	0.007	0.002	0.116	0.876

[a]The geometry of the end-on form is shown in Fig. 1.

ethylene is the outside one as shown in the above section. Based on the analyses of the net charge and the frontier density, similar reactivity is expected for the end-on superoxide species on Cu, Ag, and Au surfaces.

The reactivities of the superoxide species on Cu, Ag, and Au surface for ethylene are also very similar [39]. The differences among Cu, Ag, and Au surfaces are small, if the superoxide species exists on the metal surfaces. Large observed differences in the catalytic activity of these metal surfaces are therefore attributed to the different stabilities of the adsorbed oxygen species, particularly the stability of the superoxide species.

Next, we examine a conversion from the end-on to the side-on geometries. This process accompanies a conversion from the superoxide to the peroxide, since the ground state of the end-on and side-on species are the superoxide and peroxide, respectively, as shown in some details in this section. Thus, the method to be used here should be able to describe both ground and excited states in a good accuracy. For this purpose, the HF method is inadequate, we use the SAC/SAC-CI method [43–45]. The geometries optimized at the HF level are used for the end-on (#1) and side-on (#4) forms, respectively. The intermediate geometries #2 and #3, which are illustrated in Figure 5, are approximated as a linear function of the OMM angle.

Figure 6 shows the potential energy curves (PECs) calculated for the conversion process between the end-on and side-on forms on the Cu, Ag, and Au surfaces. In the end-on geometry, the superoxide ($^2B_2$) is always the ground state, but in the side-on geometry, the ground state is the peroxide species ($^2A_1$). The superoxide species with the $^2A_2$ symmetry is less important since it never becomes the ground state in this conversion process. In the $^2B_2$ superoxide, the in-plane π^* orbital of oxygen is singly occupied while the out-of-plane π^* orbital is doubly occupied. These occupations are reversed in the $^2A_2$ state. The crossing of the PECs of the superoxide and peroxide occurs between the end-on and side-on geometries.

Relative stabilities of the superoxide and peroxide in the end-on and side-on geometries and the barrier of the conversion are quite important for understanding the catalytic activities of metals for the epoxidation of ethylene. Such information is given in Figure 6. In the end-on form, the superoxide species is more stable than the peroxide species: the energy difference is about 20 kcal/mol for Ag and Au and 5 kcal/mol for Cu. In the side-on form, the peroxide species is more stable than the superoxide species: The energy difference is 50.1, 27.6, 21.2 kcal/mol for Cu, Ag, and Au, respectively. The energy difference between the end-on superoxide and the side-on peroxide is 50.8, 23.1, and −1.2 kcal/mol for Cu, Ag, and Au, respectively. On the Cu surface, the superoxide species in the end-on form easily converts into the peroxide species in the side-on form because of a large stabilization energy and for a lack of the barrier: The lifetime of the end-on superoxide species should be very short on the Cu surface. On the other hand, an energy barrier of about 20 kcal/mol is calculated for the conversion on Au. On the Ag surface, the end-on superoxide should have a considerable lifetime as seen from the PECs shown in Figure 6. Based on the above results, we can conclude that the reason for the nonselectivity of Cu for the epoxidation of ethylene is due to the absence of the stable adsorbed superoxide species. However, for Au, the results obtained from Figure

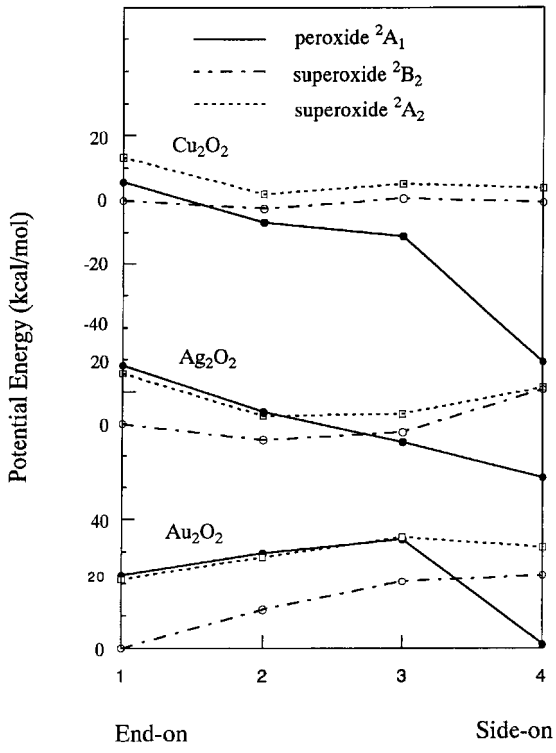

FIGURE 6. Potential energy curves calculated by the SAC / SAC-CI method for the conversion between the end-on (#1) and side-on (#4) adsorption states in the lowest three states of the Cu_2O_2, Ag_2O_2, and Au_2O_2 adclusters with $n = 1$.

6 does not give a clear explanation for its inability of this reaction. As far as one-electron transfer from the bulk metal into the adcluster occurs for Cu, Ag, and Au, the reactivity of the superoxide on these metals should be similar.

ELECTRON TRANSFERABILITY OF Cu, Ag, AND Au

The results listed in the preceding section show that the oxygen superoxide species adsorbed on Au surface has essentially the same reactivity as those on Cu and Ag surfaces. The stabilities of the molecularly adsorbed oxygen species are mainly due to the electron-transfer effect from the bulk metal as already shown previously for silver [34–36] and palladium [31, 32]. The chemical potentials (work functions) of the Cu, Ag, and Au surfaces are 4.48, 4.52, and 5.37 eV for the (110) surfaces, 4.94, 4.74, and 5.31 eV for the (111) surfaces, and 4.59, 4.64, and 5.47 eV for the (100) surfaces [47]. The Cu surface is expected to have similar properties to the Ag surface. However, it is not clear whether the electron transfer also occurs for the Au surface. We therefore investigate here the $E(n)$ curves of the M_2—O_2 systems in the DAM in order to clarify why Au cannot be a good catalyst for the epoxidation of ethylene.

Figure 7 is a display of the $E(n)$ curves, namely the energy of the adcluster calculated as a function of n. It was calculated with the use of the highest spin coupling model [39]. The optimized end-on geometries of M_2O_2 adclusters are adopted since they are the most stable geometries of the superoxide adsorbed species. The $E(n)$ curves are upper convex, and at $n = 1.0$, the systems are more stable than at $n = 0.0$, and the order of stability is $Cu_2O_2 > Ag_2O_2 > Au_2O_2$. According to DAM [31], the electron transfer would occur between the adcluster and the bulk metal when the chemical potential of the adcluster becomes equal to the chemical potential of the solid surface, i.e., $\partial E(n)/\partial n = -\mu$. For Cu_2O_2 and Ag_2O_2 systems, the tangents of the $E(n)$ curves become equal with the experimental chemical potentials at about $n = 0.9$. Therefore, from the concept of DAM [31], one electron should flow from the Cu and Ag bulk metals into the adcluster after some barrier. This is the case we used to study the activation of O_2 on the surfaces shown in the preceding section. However, for the Au_2O_2 system, though the energy at

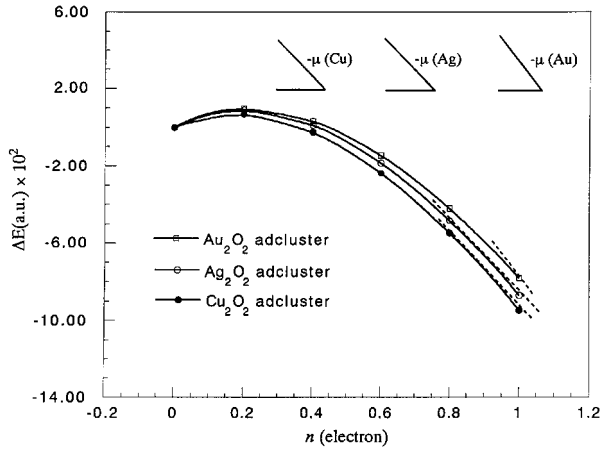

FIGURE 7. $E(n)$ curves for the Cu_2O_2, Ag_2O_2, and Au_2O_2 adclusters in the highest spin coupling model at the optimized end-on geometries.

$n = 1.0$ is lower than that at $n = 0.0$, the tangent of the $E(n)$ curve is still smaller than the experimental chemical potential. Therefore, different from Cu and Ag metals, one-electron flow does not occur from the Au metal into the adcluster. This point of the Au surface is essentially different from the other metals and should be the reason why the molecularly adsorbed oxygen species cannot exist on the clean gold surface. Thus, the inactivity of the gold surface for the oxygen is explained by the DAM as being due to its poor donating property.

The chemical potential of Au is much larger than those of Cu and Ag. We note that this difference is attributed actually to the relativistic effect in gold [48, 49]. The importance of the relativistic effects to the valence-electron properties such as chemical shift has been recently clarified in this laboratory [50–52].

We further note that the electron flow is difficult to occur between the clean gold metal and the adcluster because it does not satisfy the condition clarified by the DAM [31]. However, as the energy at $n = 1.0$ is lower than that at $n = 0.0$, the electron transfer can be realized if the chemical potentials μ of the gold metal can be lowered by an addition of promoters, etc. Experimentally, the recent works performed by Haruta et al. [53, 54] show that gold is remarkably active for the oxidation of CO and hydrocarbons when it is supported on suitable metal oxides. This may be explained by such effect of the metal-oxide support.

BRIEF SUMMARY

The electron transfer from metal to O_2 is a key factor for the chemisorption of oxygen on a metal surface, as shown previously [32–37]. The differences in the relative stabilities of different oxygen species on different metal surfaces are attributed to the differences in the electron-donating ability. The present DAM calculations show that, for Cu and Ag surfaces, one-electron transfer from the bulk metal into the adcluster occurs after some barriers. On the other hand, electron transfer is difficult to occur for the Au surface since the gold surface has the higher work function. This is why molecular adsorption of O_2 does not occur on the Au surface.

On Cu surface, peroxide is much more stable than superoxide, and there is essentially no barrier for the conversion from superoxide to peroxide, so that the lifetime of the superoxide species should be too short to react with ethylene. On Ag surface, however, the superoxide species would have considerable lifetime on the surface. On Au surface, the superoxide species does not exist because the molecular adsorption of O_2 does not occur due to the difficulty of the electron transfer from the clean bulk metal. We think that this difference in the stabilities of the end-on superoxide species on Cu, Ag, and Au surfaces is a reason of the observed difference in the catalytic activity of these metals for the epoxidation of ethylene.

The above conclusion for the origin of the different catalytic activity of Cu, Ag, and Au surfaces for the epoxidation of ethylene suggests a possibility of making a new catalyst for this reaction. The key is an appropriate lifetime of the end-on superoxide species on the metal. Silver realizes it without any special modification. However, if one can realize such superoxide species on some metals using some modification, we think that the essential factor is realized.

Oxidation Mechanism of Propylene on Silver Surface

Though silver is an effective catalyst for the epoxidation of ethylene (85–87% conversion) [5–7], it is a very poor catalyst for the epoxidation of propylene (2–5% conversion) [12–16]. A relatively small substitution of hydrogen with methyl group,

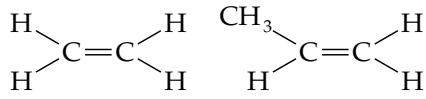

causes such a drastic change of the reaction. It is interesting to understand why. To know the difference of the oxidation mechanism between ethylene and propylene will lead to a better understanding of the general oxidation mechanism of other olefins on silver surface. Further, in the chemical industry, propylene oxide is an important material, so that to know why silver is so poor for the conversion of propylene to propylene oxide is a starting point for a design of a new effective catalyst. This section is a summary of our recent study on the oxidation mechanism of propylene [40].

Two possible reasons may be considered for the difference in the reaction of ethylene and propylene on a silver surface. One possibility is that the reaction routes are the same but the methyl substituent causes a large change in the barrier height and/or in the stability of the intermediates in the course of the reaction. Another possibility is that an entirely different reaction route comes out for the existence of the methyl group. We have investigated these two possibilities. As in the case of ethylene, we study the reactions of the two active oxygen species on a silver surface: the molecularly adsorbed superoxide species and the dissociatively adsorbed atomic oxygen species.

The calculational methods are the same as those discussed in the second section. The DAM [31–33] was used to include the effect of the bulk metal such as the electron transfer and the image force. The basis sets are the same as before, and the geometries of the reactants, intermediates, transition states, and the products were optimized by the Hartree–Fock method and the energies were calculated by the MP2 method in order to include the effects of electron correlations.

ATTACK ON OLEFINIC CARBON

We first study the reaction route, which is essentially the same as that of ethylene [38]: The reaction starts from the interaction between the adsorbed oxygen and the doubly bonded carbon atom of propylene. Figure 8 is an illustration of the adcluster for the initial interaction of propylene

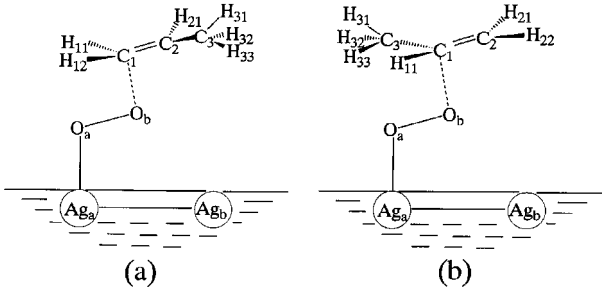

FIGURE 8. Model adclusters for the olefinic carbon attack mechanism: (a) on the terminal olefinic carbon, (b) on the central olefinic carbon.

with the superoxide species. Since two carbons in propylene are different, two different attacks were considered. The interaction with atomic oxygen was similarly considered. The reaction may process as follows:

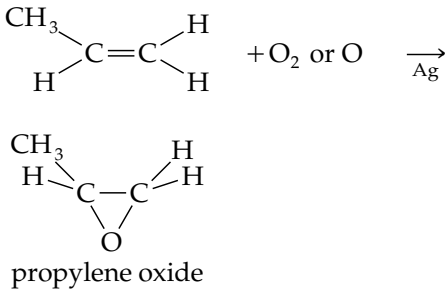

(2)

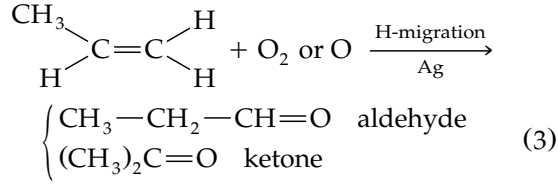

(3)

In (3), aldehyde is a product of the terminal C attack and ketone is a product of the central C attack, and they are further oxidized to CO_2 and H_2O.

Figure 9 shows the optimized geometries and the energy diagrams for the reaction of the molecularly adsorbed oxygen with the terminal C of propylene. It is similar to Figure 2 for the reaction with ethylene: The substitution of one hydrogen with methyl group does not cause a large change for the reaction route and the energetics. In this reaction mechanism, the route going to propylene oxide should be quite smooth without any high-energy barrier and without any too stable intermediate, while the route leading to the aldehyde should be essentially blocked up by the existence of a high-energy barrier in the hydrogen migration step. The diagram for the reaction of the superoxide with the central carbon atom of propylene [Fig. 8(b)] was similar to Figure 9 [40]. Thus, if the reaction proceeds along this reaction route, propylene oxide should be produced in high selectivity due to the catalytic activity of the superoxide

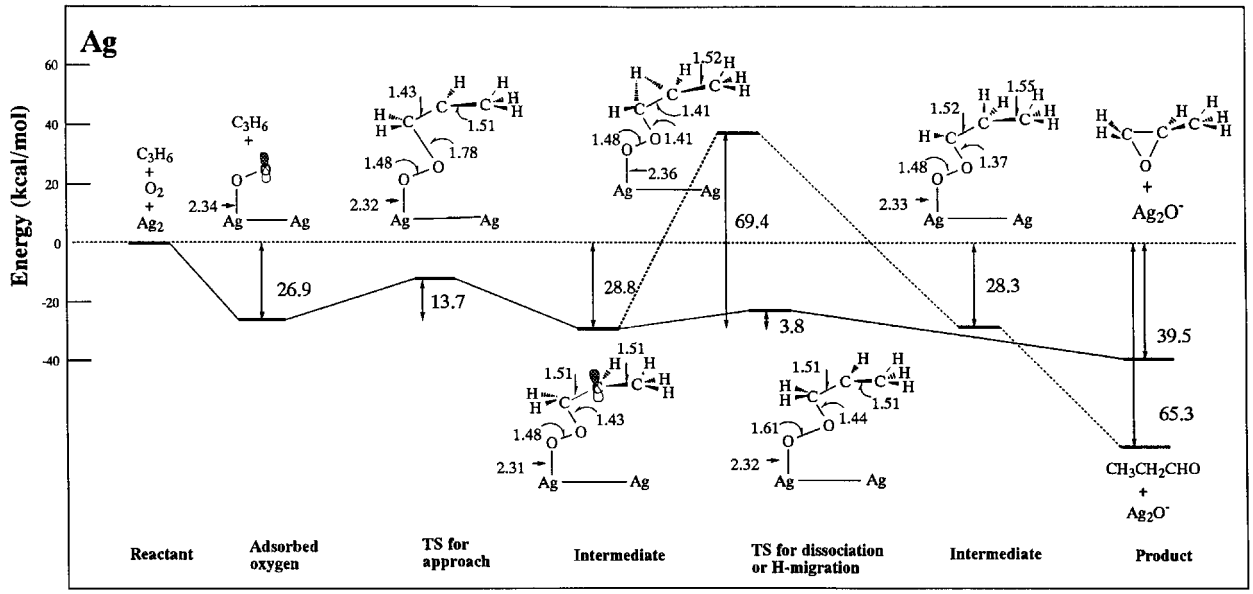

FIGURE 9. Energy diagram for the reaction between the terminal carbon atom of propylene and the molecularly adsorbed superoxide on a Ag surface. The route leading to propylene oxide and aldehyde are shown by the solid and broken lines, respectively.

species adsorbed on silver. Also, for the reaction with atomically adsorbed oxygen, a similar conclusion as that of ethylene may be obtained as the reaction route and the energy diagrams of propylene are similar to ethylene [38].

The results shown above mean that if the reaction proceeds through the oxygen attack on the olefinic carbon of propylene, silver should be as good a catalyst as for ethylene for the epoxidation. However, this result contradicts with the experimental observation that the conversion of propylene into propylene oxide is only 2–5% on the silver catalyst [12–17]. We therefore examine another possibility that a reaction route entirely different from those of ethylene may exist. Since propylene has a methyl group, but ethylene does not, we next examine the reaction route involving the reaction of this methyl group with the reactive oxygen on a silver surface.

ATTACK ON ALLYLIC HYDROGEN

Propylene is different from ethylene by an existence of a methyl group. We examine here the reaction route involving the reaction of this methyl group with the superoxide and the atomic oxygen on a silver surface. Figure 10 shows the initial attack of the superoxide [Fig. 10(a)] and atomic oxygen [Fig. 10(b)] on the methyl hydrogen, and the reactions process as follows:

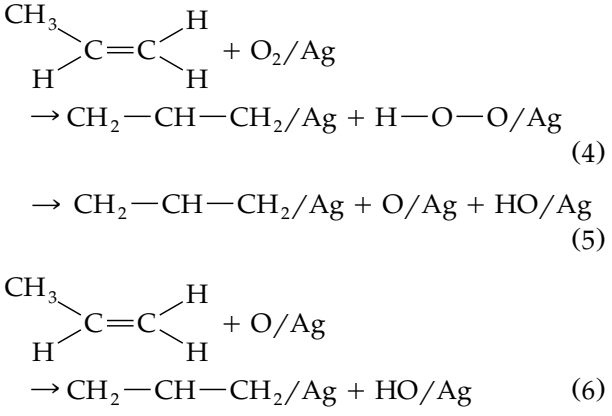

These reactions produce the allyl intermediate adsorbed on the silver surface, which is oxidized further to CO_2 and H_2O. Since allyl radical or anion is a rather stable intermediate, this reaction route is feasible.

Figure 11 shows the optimized reaction route for the attack of superoxide on the methyl hydrogen of propylene as given by (4) and (5). The present result was added to the previous one for

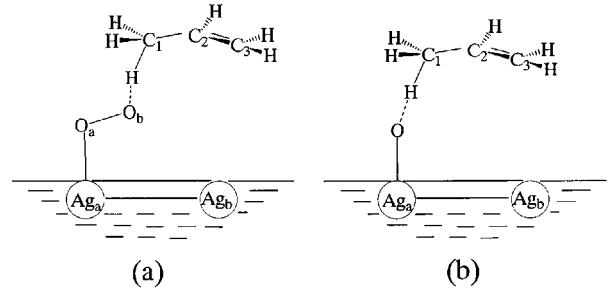

FIGURE 10. Model adclusters for the allylic H attack mechanism: (a) reaction with molecularly adsorbed superoxide species, (b) reaction with atomically adsorbed oxygen.

the carbon attack given in Figure 9. The optimized geometries of the intermediates and the transition states for the present H attack are given in the lower side, while those for the previous C attack are given on the upper side. The energy levels of the intermediates and the transition states for the present reaction route are lower than those of the previous one. The barrier for the attack on the methyl hydrogen was calculated to be 10.8 kcal/mol, which is lower than the barrier for the carbon attack, 13.7 kcal/mol, and then the system becomes allyl intermediate and the hydroperoxy group adsorbed on silver [Eq. (4)]. This intermediate is also more stable than the previous one, but the hydroperoxy group is unstable and further converted into OH and O as given by Eq. (5): The barrier in this step is only 2.8 kcal/mol and the stabilization energy is as large as 42.6 kcal/mol. When two-site interaction between allyl and silver surface is further allowed, the system is further stabilized by 18.1 kcal/mol. Thus, the reaction route starting from the allylic H attack is always lower than that starting from the olefinic C attack, so that the reactions represented by Eqs. (4) and (5) should proceed more easily than the reactions given by Eqs. (2) and (3).

We next examine the similar reaction given by Eq. (6) involving the atomic oxygen adsorbed on silver. Figure 12 shows the optimized reaction route and its energetics. The lower figures give the optimized geometries for the allylic H attack and the upper ones for the olefinic C attack. The barrier for the allylic H attack is essentially zero: only 0.1 kcal/mol. The allyl intermediate is more stable than the intermediate of the previous C attack: when two-site interaction between allyl and silver surface is allowed, it is further stabilized by 18.1 kcal/mol. Thus, again, for the atomic oxygen on

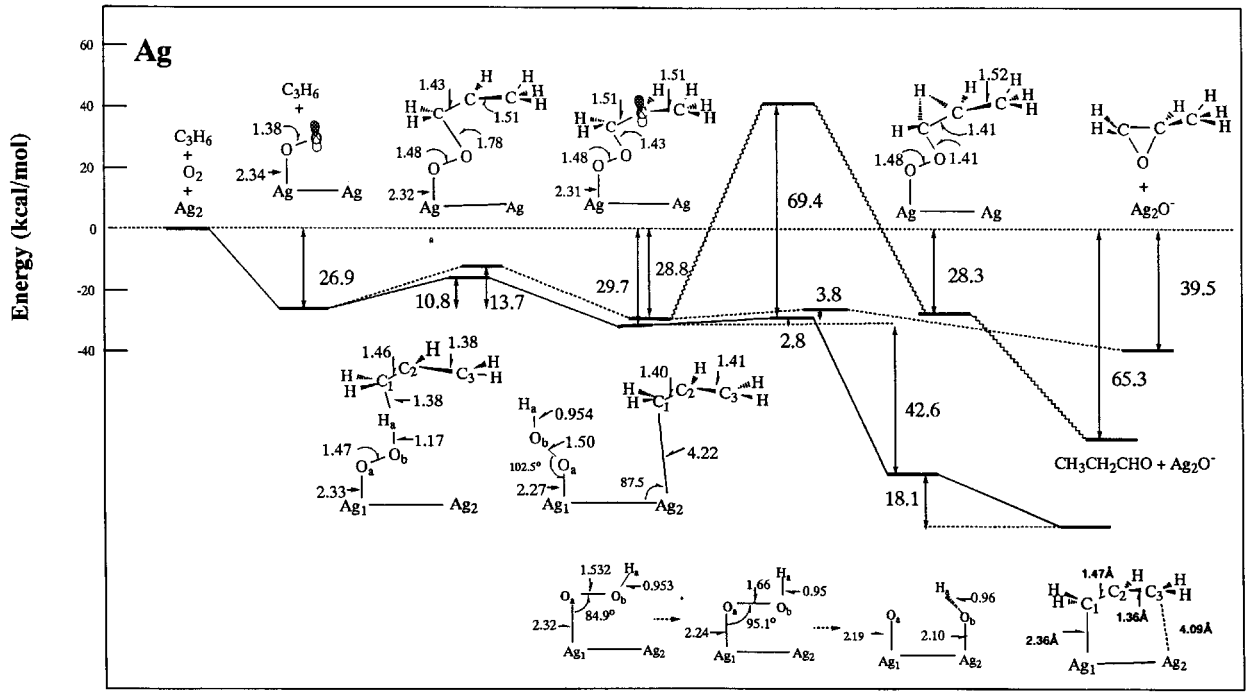

FIGURE 11. Comparison of the energy diagrams for the reactions between propylene and the molecularly adsorbed oxygen. The route for the allylic H attack is shown by the solid line, and those for the carbon attack are shown by the broken and waved lines.

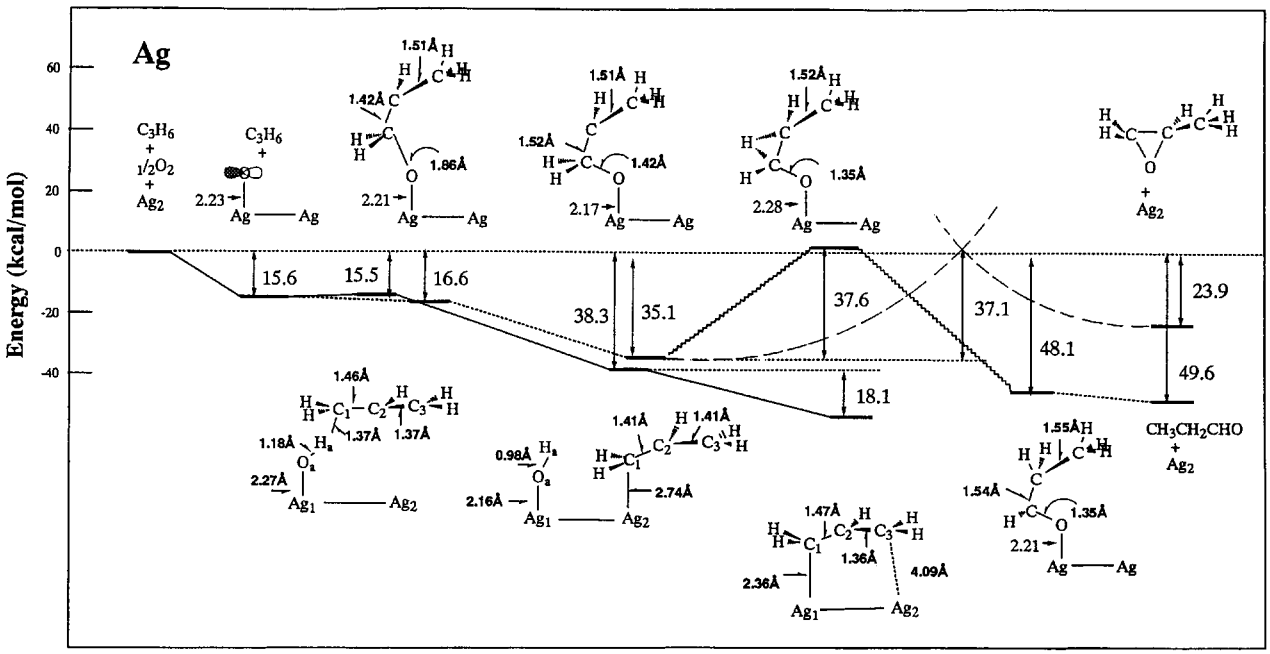

FIGURE 12. Comparison of the energy diagrams for the two reactions between propylene and the atomically adsorbed oxygen on a Ag surface.

the silver surface, the allylic H attack is an easier reaction than the olefinic C attack. The allyl intermediate thus produced is stable on the silver surface so that it will be further attacked by the oxygen species on the surface and would finally be converted into CO_2 and H_2O.

Thus, for both superoxide and atomic oxygen on a silver surface, the reaction starting from the allylic H attack proceeds more easily than the one starting from the olefinic C attack. Therefore, the conversion to propylene oxide does not effectively occur on a silver surface.

The origin of the activation of this allyl hydrogen is due to the stability of the preceding adsorbed allyl intermediate. We have investigated the nature of the allyl intermediate adsorbed on a silver surface. Figure 13 shows the optimized geometry of the allyl intermediate on Ag_2 calculated with $n = 0$ and $n = 1$. We see that the adsorption energy is larger with $n = 1$ than with $n = 0$, indicating that the allyl species on silver is actually an allyl anion species. Actually, the charge on the allyl group was -0.52 for $n = 1$, while it was -0.27 in the case of $n = 0$. The existence of the anion allyl species on silver surface had been suggested experimentally by Madix et al. [23] to be the intermediate leading to the complete oxidation.

BRIEF SUMMARY

Figure 14 is a summary of the reaction mechanism of propylene on a silver surface. The allylic hydrogen is more reactive than the olefinic carbon, due to the stability of the allyl anion species on the silver surface, so that propylene is converted to allyl intermediate and further converted to CO_2 and H_2O. If an olefin does not have an allylic hydrogen, like ethylene, styrene, etc., it is converted to epoxide in high selectivity. Even if it has an allylic hydrogen but the allyl intermediate is not stable like in norbornene, the route leading to epoxide is more preferable. This explains the selectivity of the silver surface for the epoxidation reactions of olefins.

We note that the present results clearly show that the route leading to propylene oxide also exists on a silver surface. However, it is not the most favorable reaction path. The selectivity is just between 2 and 5% experimentally. Since propylene oxide is an important material in chemical industry, it is interesting whether we can block up the route leading to the allylic intermediate.

Concluding Remarks

We reported, in this study, the mechanisms of the epoxidation and complete oxidation reaction of propylene on a silver surface and the stabilities and activities of the oxygen species adsorbed on Cu, Ag, and Au surfaces. We performed the (U)HF, MP2, and SAC/SAC-CI calculations with the use of the DAM which involved the interaction between bulk metal and admolecules with consideration of electron transfer and image force correction.

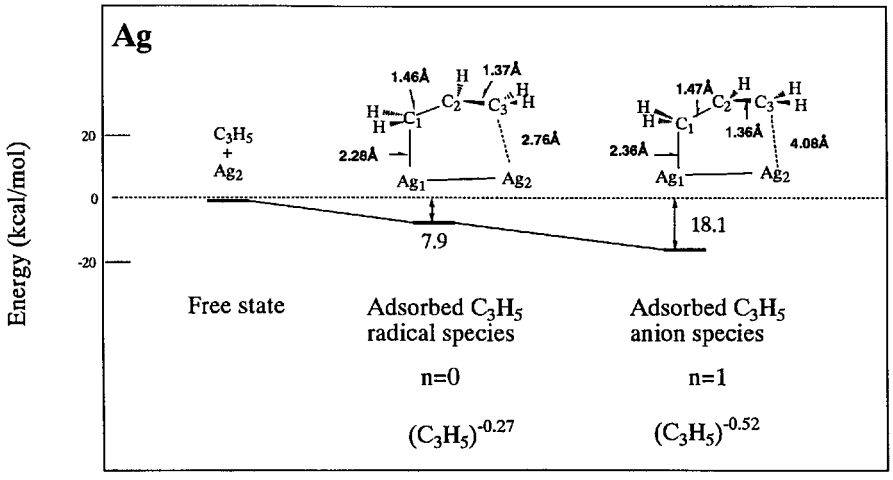

FIGURE 13. Stability of the allyl species adsorbed on Ag_2 cluster in the neutral ($n = 0$) and anion ($n = 1$) adcluster states.

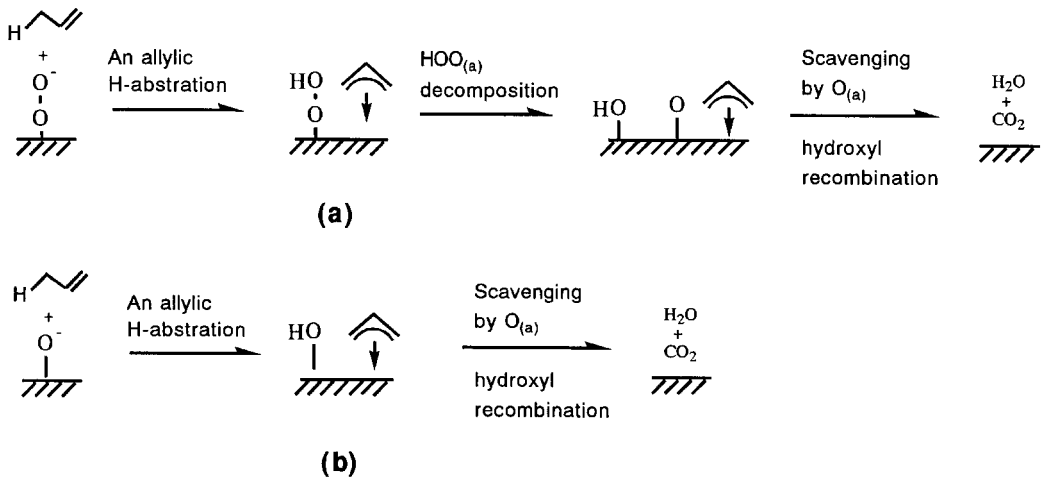

FIGURE 14. Mechanism of the complete oxidation of propylene over a silver surface; (a) with molecularly adsorbed oxygen, (b) with atomically adsorbed oxygen.

For the epoxidation of ethylene, the active species is the superoxide, which is molecularly adsorbed on the surface in the bent end-on geometry. Ethylene attacks the terminal oxygen atom of the superoxide leading to ethylene oxide quite smoothly. The importance of the silver surface is quite evident. On the other hand, the atomically adsorbed oxygen species is not selective: Both epoxidation and complete oxidation products would be obtained. However, to promote the selectivity of the atomically adsorbed species will certainly promote the total selectivity to epoxidation product. In the process leading to ethylene oxide, the electron back-transfer from the reaction adsorbate complex to the metal surface should be important.

The origin of the catalytic activity of the silver surface is due to its ability to stabilize the superoxide species. On Cu surfaces, peroxide is much more stable than superoxide, so that the lifetime of the superoxide species should be too short to react with ethylene. On Au surfaces, the superoxide species does not exist because the molecular adsorption of O_2 does not occur due to the difficulty of the electron transfer from the clean bulk metal.

For the oxidation of propylene on silver surface, two competitive mechanisms exist. The dominant mechanism for the epoxidation of olefins is initiated by the activation of the olefinic carbon. The dominant mechanism for the complete oxidation of propylene is due to the activation of the allylic C—H bond. The latter is more favorable due to the formation of the stable adsorbed allyl intermediate, which is the motivation force for the complete oxidation of propylene.

We note that the proposed two competitive mechanisms not only reflect the difference between ethylene and propylene but also explain rather well the available experimental facts for the epoxidation and complete oxidation of olefins. Therefore, it reflects a general mechanism to understand the oxidation of olefins over silver surface.

ACKNOWLEDGMENTS

Some calculations were performed using the computers at the Institute for Molecular Science. Part of this study was supported by a Grant-in-Aid for Scientific Research from the Japanese Ministry of Education, Science, and Culture and by the New Energy and Industrial Technology Development Organization (NEDO).

References

1. R. A. van Santen and H. P. C. E. Kuipers, Adv. Catal. **35**, 265 (1987).
2. W. M. H. Sachtler, C. Backx, and R. A. van Santen, Cat. Rev. Sci. Eng. **23**, 127 (1981).
3. X. E. Verykios, F. P. Stein, and R. W. Coughlin, Cat. Rev. Sci. Eng. **22**, 197 (1980).
4. K. A. Jørgensen, Chem. Rev. **89**, 431 (1989).
5. A. Ayame, in *Series of Lectures on Catalysis VII, Fundamental Industrial Catalytic Reactions*, Murakami Y, Ed. (Catalytic Society of Japan, Tokyo, 1985), pp. 170–185, in Japanese.

6. A. Ayame and H. Kanoh, Shokubai **20**, 381 (1978), in Japanese.
7. H. Miura, A. Ayame, H. Kanoh, K. Miyahara, and I. Toyoshima, Shinku **25**, 302 (1982).
8. Y. Murakomo and K. Tanaka, Nippon Kagaku Kaishi **11**, 1603 (1977).
9. S. Hawker, C. Mukoid, J. P. S. Badyal, and R. M. Lambert, Surf. Sci. **219**, L615 (1989).
10. C. Mukoid, S. Hawker, J. P. S. Badyal, and R. M. Lambert, Catal. Lett. **4**, 57 (1990).
11. J. T. Roberts and R. J. Madix, J. Am. Chem. Soc. **110**, 8540 (1988).
12. N. W. Cant and W. K. J. Hall, J. Catal. **52**, 81 (1978).
13. M. Imachi, M. Egashira, R. L. Kuczkowski, and N. W. Cant, J. Catal. **70**, 177 (1981).
14. C. Henriques, M. F. Portela, C. Mazzocchia, and E. Guglielminotti, *New Frontiers in Catalysis*, L. Guczi et al., Eds. (Elsevier, Amsterdam, 1993), p. 1995.
15. P. V. Geenen, H. J. Boss, and G. T. Pott, J. Catal. **77**, 499 (1982).
16. M. Akimoto, K. Ichikawa, and E. Echigoya, J. Catal. **76**, 333 (1982).
17. C. T. Campbell, J. Catal. **157**, 43 (1985); **99**, 28 (1986).
18. C. T. Campbell and M. T. Paffett, Surf. Sci. **143**, 517 (1984); **177**, 417 (1986).
19. E. L. Force and A. T. Bell, J. Catal. **38**, 440 (1975); **40**, 356 (1975).
20. R. B. Grant and R. M. Lambert, J. Catal. **92**, 364 (1985).
21. J. T. Gleaves, A. G. Sault, R. J. Madix, and J. R. Ebner, J. Catal. **121**, 202 (1990).
22. M. A. Barteau and R. J. Madix, J. Am. Chem. Soc. **105**, 344 (1983).
23. J. T. Roberts, R. J. Madix, and W. W. Crew, J. Catal. **141**, 300 (1993).
24. H. H. Voge and C. R. Adams, Advan. Catal. **17**, 151 (1967).
25. M. Kobayashi, M. Yamamoto, and H. Kobayashi, *Proc. 6th. Intern. Congr. Catal.* A24, 1976; M. Kobayashi, *Catalysis Under Transient Conditions*, A. T. Bell and L. L. Hegedus, Eds. (ACS, Washington, DC, 1982), p. 209.
26. J. Deng, J. Yang, S. Zhang, and X. Yuan, J. Catal. **138**, 395 (1992).
27. E. A. Carter and W. A. Goddard, J. Catal. **112**, 80 (1988); Surf. Sci. **209**, 243 (1989).
28. P. J. van den Hoek, E. J. Baerends, and R. A. van Santen, J. Phys. Chem. **93**, 6469 (1989).
29. K. A. Jørgenson and R. Hoffmann, J. Phys. Chem. **94**, 3046 (1990).
30. S. Beran, P. Jiru, B. Wichterlova, and R. Zahradnik, *Proc. Sixth Int. Cobgr. Catal.* **1**, 324 (1997).
31. H. Nakatsuji, J. Chem. Phys. **87**, 4995 (1987).
32. H. Nakatsuji, H. Nakai, and Y. Fukunishi, J. Chem. Phys. **95**, 640 (1991).
33. H. Nakatsuji, Proc. Surf. Sci. **54**, 1 (1997).
34. H. Nakatsuji and H. Nakai, Chem. Phys. Lett. **174**, 283 (1990).
35. H. Nakatsuji and H. Nakai, J. Chem. Phys. **98**, 2423 (1993).
36. H. Nakatsuji and H. Nakai, Can. J. Chem. **70**, 404 (1992).
37. H. Nakatsuji, Int. J. Quant. Chem. **42**, 725 (1992).
38. H. Nakatsuji, H. Nakai, K. Ikeda, and Y. Yamamoto, Surf. Sci., in press.
39. H. Nakatsuji, Z. M. Hu, H. Nakai, and K. Ikeda, Surf. Sci., in press.
40. Z. M. Hu, H. Nakai, and H. Nakatsuji, Surf. Sci., submitted.
41. X. Bao, J. Deng, and S. Dong, Surf. Sci. **163**, 444 (1985).
42. L. Ya. Margolis, Adv. Catal. **14**, 4289 (1963).
43. H. Nakatsuji and K. Hirao, J. Chem. Phys. **68**, 2053 (1978).
44. H. Nakatsuji, Chem. Phys. Lett. **59**, 362 (1978); **67**, 329 (1979).
45. H. Nakatsuji, in *Computational Chemistry—Reviews of Current Trends*, J. Leszczynski, Eds. (World Scientific, London, 1997).
46. P. H. Krupenie, J. Phys. Chem. Ref. Data **1**, 423 (1972).
47. *Handbook of Chemistry and Physics*, R. C. Weast et al., Eds. (CRC Press, Cleveland, 1984–1985).
48. E. Eliav, U. Kaldor, and Y. Ishikawa, Phys. Rev. A **49**, 1724 (1994).
49. U. Kaldor and B. A. Hess, Chem. Phys. Lett. **230**, 1 (1994).
50. H. Nakatsuji, H. Takashima, and M. Hada, Chem. Phys. Lett. **233**, 13; 95 (1995).
51. C. C. Ballard, M. Hada, H. Kaneko, and H. Nakatsuji, Chem. Phys. Lett. **254**, 170 (1996).
52. H. Nakatsuji, M. Hada, H. Kaneko, and C. C. Ballard, Chem. Phys. Lett. **255**, 195 (1996).
53. M. Haruta, S. Tsubota, T. Kobayashi, M. Kageyama, M. Genet, and B. Delmon, J. Catal. **144**, 175 (1993).
54. T. Hayashi and M. Haruta, Shokubai 37 (1995) 72, in Japanese; M. Haruta, Chem. Eng. **59**, 168 (1995), in Japanese.